



---

*Research article*

## Sensitivity analysis and optimal treatment control for a mathematical model of Human Papillomavirus infection

Kai Zhang<sup>1</sup>, Yunpeng Ji<sup>2,3,4</sup>, Qiuwei Pan<sup>2,3</sup>, Yumei Wei<sup>5</sup>, Yong Ye<sup>1</sup> and Hua Liu<sup>1,\*</sup>

<sup>1</sup> School of Mathematics and Computer Science, Northwest Minzu University, Lanzhou 730030, P. R. China

<sup>2</sup> Biomedical Research Center, Northwest Minzu University, Lanzhou, P. R. China

<sup>3</sup> Department of Gastroenterology and Hepatology, Erasmus MC-University Medical Center, Rotterdam, The Netherlands

<sup>4</sup> Department of Genetics, Inner Mongolia Maternal and Child Care Hospital, Hohhot, Inner Mongolian Autonomous Region, P. R. China

<sup>5</sup> Experimental Teaching Department, Northwest Minzu University, Lanzhou 730030, P. R. China

\* **Correspondence:** Email: 7783360@qq.com.

**Abstract:** Human papillomavirus (HPV) is one of the most common sexually transmitted viruses, and is a causal agent of cervical cancer. We aimed to develop a mathematical model of HPV natural history and qualitatively analyzed the stability of disease-free equilibrium, non-existence of limit cycle and existence of forward bifurcation. We performed sensitivity analysis to identify key epidemiological parameters. The Partial Rank Correlation Coefficient (PRCC) values for basic reproduction number shows that controlling contact rate plays an important role in disturbing equilibrium of HPV infection. Moreover, the increase of medical level is the most effective measure to prevent new HPV infections. Optimal treatment problem is solved and theoretical analysis is verified by numerical simulation.

**Keywords:** HPV-disease; forward bifurcation; sensitivity analysis; optimal control; numerical simulations

**Mathematics Subject Classification:** 92C60, 92D30

---

### 1. Introduction

Although the majority of human papillomavirus (HPV) infections are transient and thus are

relatively harmless, persistent infection with certain high-risk HPV genotypes can cause cervical precursor lesions and cervical carcinoma [1,2]. Cervical cancer is the most common malignancy reported among women in developing countries and is a leading cause of cancer deaths worldwide, with an estimated 233,000 deaths in 2000 [3]. By 2002, the number of women dying from cervical cancer had risen to 274,000 [4–6]. Nearly, all cervical cancers are attributable to genital infection with HPV [7,8]. Up to 70% of women in the general population will acquire genital HPV infection during their lifetime [9]. Most HPV related infections are cleared by treatment or natural healing of the host, while some are persistent and may develop into cervical cancer [10,11]. The progression from persistent infection to cervical cancer typically needs a period of 20 years or longer [12,13]. Fortunately, therapeutic HPV vaccines have made progress in clinical trials after long-term exploration and development. These vaccines include DNA vaccines, RNA replicon vaccines, peptide vaccines, vector vaccines, cell vaccines, and protein vaccines [14,15].

Mathematical models have been established to understand the dynamics of HPV related disease. In the modeling, some important variables specific for infectious disease are developed. For example, a variable representing how often an infectious individual contacts with a susceptible individual in a unit time is defined as the contact rate. The probability of each contact is set as  $\beta$ , indicating the ability of an infectious person to infect others (susceptible persons) in unit time. Considering that there are other members (e.g., immune persons  $R(t)$ ), and that the number of members infected by one infected person in a unit time is limited, let  $N(t) = S(t) + I(t) + R(t)$ , where the total population  $N(t)$  is divided into three epidemiological states:  $S(t)$  is size of the susceptible population at time  $t$  and  $I(t)$  is size of the infected population at time  $t$ . This generates a formula for the incidence rate: the standard incidence rate  $\frac{\beta S(t)I(t)}{N(t)}$  represents the newly infected

individuals infected by infectious individuals in unit time at time  $t$ . Based on these studies, A Omame et al [16] formulated a mathematical model to investigate the impact of treatment and vaccination on HPV transmission dynamics. Elamin H and Elbasha et al [17] developed a nonlinear, deterministic and age-structured mathematical model. In the same year, Elamin H and Elbasha [18] studied the dynamic behaviors of a two-sex, deterministic model for assessing the potential impact of a prophylactic HPV vaccine with several properties. Mo'tassem and S Robert [19] developed an age-dependent two-sex mathematical model to describe the HPV vaccination program for a vaccine targeting HPV types 16 and 18 in both childhood and adult stages.

With the development of the mathematical model used to explain the spread of infectious diseases, optimization strategies are introduced into the model. Eihab B M et al [20] studied an optimal control model governed by a system of delay differential equations. The optimal vaccination strategy for a constrained time-varying SEIR (Susceptible, Exposed, Infected and Recovered) epidemic model was solved [21]. T K Kar and Ashim Batabyal [22] formulated a nonlinear mathematical SIR epidemic model with a vaccination program. Yang and Tang et al [23] studied a mathematical model to explore the impact of vaccination and treatment on the transmission dynamics of tuberculosis (TB).

The purpose of this study was to incorporate both therapeutic HPV vaccines and partial immunity compartments based on the present models to investigate how they influence dynamic behavior and to further examine the optimal treatment control measures to minimize the number of asymptomatic patients and treatment costs. We formulate a mathematical model for HPV transmission, and the existence and stability of the equilibria are discussed. In the next section, we present a sensitivity analysis of the model through Partial Rank Correlation Coefficients to identify

the key factors in the model. After that, we use optimal control and theory to minimize the number of asymptomatic patients and treatment costs; we also carry out some numerical simulations to highlight the effect of optimal treatment control on the model. Finally, we give concluding remarks.

## 2. A HPV model with treatment

### 2.1. Model formulation

Since persistent infection with high-risk HPV genotypes is the main cause of precursor cervical lesions and cervical carcinoma [24], we divided a cohort into three groups, namely, asymptomatic infectious individuals ( $E$ ), symptomatic infectious females or males ( $I_1$ ), and individuals with persistent HPV infection ( $I_2$ ). The persistently infected individuals who have not been treated will develop cervical cancer ( $A$ ) after a period of time. Moreover, we consider that  $E$ ,  $I_1$ ,  $I_2$  can be cured and become recovered ( $R$ ), thus gaining permanent or temporary immunity, which is less reported in previous studies (Table 1). Our assumptions for the dynamic transmission of HPV are demonstrated in Figure 1.

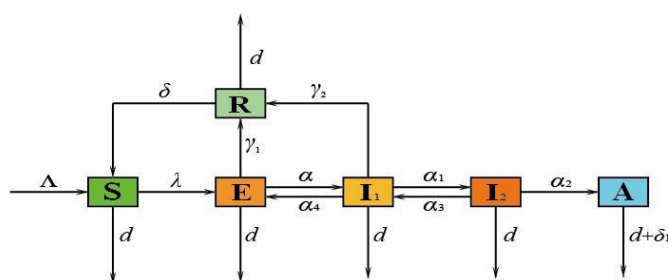


**Figure 1.** Flow chart of the HPV transmission.

The total human population at time  $t$ , denoted by  $N(t)$ , is subdivided into 6 mutually exclusive compartments of  $S$ ,  $E$ ,  $I_1$ ,  $I_2$ ,  $A$ ,  $R$ . Thus

$$N(t) = S(t) + E(t) + I_1(t) + I_2(t) + A(t) + R(t). \quad (2.1)$$

Combining all the aforementioned definitions and assumptions, it follows that the model for the transmission dynamics of HPV in a population is given by the following system of nonlinear differential equations:

$$\begin{cases} \frac{dS}{dt} = \Lambda + \delta R(t) - \lambda(t)S(t) - dS(t), \\ \frac{dE}{dt} = \lambda(t)S(t) + \alpha_4 I_1(t) - (\alpha + \gamma_1 + d)E(t), \\ \frac{dI_1}{dt} = \alpha E(t) + \alpha_3 I_2(t) - (\alpha_1 + \alpha_4 + \gamma_2 + d)I_1(t), \\ \frac{dI_2}{dt} = \alpha_1 I_1(t) - (\alpha_3 + \alpha_2 + d)I_2(t), \\ \frac{dA}{dt} = \alpha_2 I_2(t) - (\delta_1 + d)A(t), \\ \frac{dR}{dt} = \gamma_1 E(t) + \gamma_2 I_1(t) - (\delta + d)R(t), \end{cases} \quad (2.2)$$

where

$$\lambda(t) = \frac{\beta_1 E(t) + \beta_2 I_1(t) + \beta_3 I_2(t)}{N(t)}. \quad (2.3)$$

**Table 1.** Description of variables and parameters in the model.

Variable	Description
$S(t)$	Susceptible individuals
$E(t)$	Infectious individuals with no symptoms
$I_1(t)$	Individuals with HPV symptoms
$I_2(t)$	Individuals with persistent infection
$A(t)$	Cancer-infected individuals
$R(t)$	Recovered individuals
Parameter	Description
$\Lambda$	Rate of recruitment
$d$	Natural mortality rate
$\delta_1$	Disease-induced mortality for individuals
$\delta$	Rate at which recovered individuals become susceptible
$\beta_1$	Probability of infection in contact with no symptom persons
$\beta_2$	Probability of infection in contact with infectious individuals
$\beta_3$	Probability of infection in contact with persistent infections individuals
$\alpha$	Rate of progression to symptomatic stage for individuals
$\alpha_1$	Rate at which symptomatic individuals become persistent infections
$\alpha_2$	Rate at persistent HPV infection develops cervical cancer
$\alpha_3$	Rate from persistent infections to symptomatic stage
$\alpha_4$	Rate from symptomatic stage to no symptom stage
$\gamma_1$	Rate of recovery from persistent infections
$\gamma_2$	Rate of recovery from no symptom stage

## 2.2. Positivity and boundedness of solutions

Here, we shall show the positivity and boundedness of the population.

**Lemma 1.** [25] Assume that  $x(t)$  satisfies  $x(0) > 0$  and  $a > 0$ ,  $b > 0$ ,  $\frac{dx}{dt} \leq b - ax$ , then

$$\limsup_{t \rightarrow \infty} x(t) \leq \frac{b}{a}.$$

**Theorem 1.** Let  $S(0) \geq 0$ ,  $E(0) \geq 0$ ,  $I_1(0) \geq 0$ ,  $I_2(0) \geq 0$ ,  $A(0) \geq 0$ ,  $R(0) \geq 0$ , then the solutions  $S(t)$ ,  $E(t)$ ,  $I_1(t)$ ,  $I_2(t)$ ,  $A(t)$ ,  $R(t)$  are positive for all  $t > 0$ .

**Proof** It follows from the first equation of the system (2.2) that

$$\frac{dS}{dt} = \Lambda + \delta R(t) - \lambda(t)S(t) - dS(t),$$

which can be re-written as

$$\frac{d}{dt} \left\{ S(t) \exp \left[ \int_0^t \lambda(\rho) d\rho + dt \right] \right\} = (\Lambda + \delta R) \exp \left[ \int_0^t \lambda(\rho) d\rho + dt \right],$$

hence

$$S(t) \exp \left[ \int_0^t \lambda(\rho) d\rho + dt \right] - S(0) = \int_0^t (\Lambda + \delta R) \exp \left[ \int_0^\theta \lambda(\theta) d\theta + d\theta \right] d\theta,$$

so that

$$\begin{aligned} S(t) &= S(0) \exp \left[ - \int_0^t \lambda(\rho) d\rho + dt \right] \\ &\quad + \int_0^t (\Lambda + \delta R) \exp \left[ \int_0^\theta \lambda(\theta) d\theta + d\theta \right] d\theta \\ &> 0. \end{aligned}$$

Similarly, it can be shown that  $E(t) \geq 0$ ,  $I_1(t) \geq 0$ ,  $I_2(t) \geq 0$ ,  $A(t) \geq 0$ ,  $R(t) \geq 0$ .

**Theorem 2.** The region  $\Omega$  is positively invariant for model (2.2) with initial conditions in  $R_+^6$ .

**Proof** Adding all the equations in the differential equation system (2.2) gives

$$\frac{dN}{dt} \leq \Lambda - dN, \quad (2.4)$$

by using Lemma 1, one could easily obtain that

$$N(t) \leq \frac{\Lambda}{d} + N(0) \exp(-dt),$$

when  $t \rightarrow \infty$ , we have

$$N(t) \leq \frac{\Lambda}{d}.$$

Let

$$\Omega = \left\{ (S, E, I_1, I_2, A, R) \in R_+^6 \mid S, E, I_1, I_2, A, R \geq 0, S + E + I_1 + I_2 + A + R \leq \frac{\Lambda}{d} \right\},$$

the region  $\Omega$  is positively invariant.

In this region, the model can be considered as been epidemiologically and mathematically well-posed [26]. Thus, each solution of the basic model (2.2) with initial conditions in  $\Omega$  remains in  $\Omega$  for all  $t > 0$ .

### 2.3. Stability analysis

The model (2.2) has a disease-free equilibrium (DFE), given by

$$x_0 = (S_0, E_0, I_{01}, I_{02}, A_0, R_0) = \left( \frac{\Lambda}{d}, 0, 0, 0, 0, 0 \right).$$

Let  $X = (E, A, I_2, I_1, S, R)$ , using the notation [27], the model consists of nonnegative initial conditions together with the following system of equations:

$$\frac{dX}{dt} = \Phi(X) - \Gamma(X),$$

where

$$\Phi(X) = \begin{pmatrix} \frac{\beta_1 SE + \beta_2 SI_1 + \beta_3 SI_2}{N} \\ N \\ 0 \\ 0 \\ 0 \\ 0 \\ 0 \\ 0 \end{pmatrix}, \quad \Gamma(X) = \begin{pmatrix} -\alpha_4 I_1 + a_1 E \\ -\alpha_2 I_2 + a_4 A \\ -\alpha_1 I_1 + a_3 I_2 \\ -\alpha E - \alpha_3 I_2 + a_2 I_1 \\ -\Lambda + \frac{\beta_1 SE + \beta_2 SI_1 + \beta_3 SI_2}{N} - \delta R + dS \\ -\gamma_1 E - \gamma_2 I_1 + (\delta + d)R \end{pmatrix},$$

and  $a_1 = \alpha + \gamma_1 + d$ ,  $a_2 = \alpha_1 + \alpha_4 + \gamma_2 + d$ ,  $a_3 = \alpha_3 + \alpha_2 + d$ ,  $a_4 = \delta_1 + d$ ,  $a_5 = d + \delta$ . It is obvious that

$$D\Phi(x_0) = \begin{pmatrix} F & 0 \\ 0 & 0 \end{pmatrix}, \quad D\Gamma(x_0) = \begin{pmatrix} V & 0 \\ J_3 & J_4 \end{pmatrix},$$

the matrices  $F$  and  $V$ , for the new infection terms and the remaining transfer terms, are, respectively, given by

$$F = \begin{pmatrix} \frac{\beta_1 S_0}{N} & 0 & \frac{\beta_3 S_0}{N} & \frac{\beta_2 S_0}{N} \\ 0 & 0 & 0 & 0 \\ 0 & 0 & 0 & 0 \\ 0 & 0 & 0 & 0 \end{pmatrix}, \quad V = \begin{pmatrix} a_1 & 0 & 0 & -\alpha_4 \\ 0 & a_4 & -\alpha_2 & 0 \\ 0 & 0 & a_3 & -\alpha_1 \\ -\alpha & 0 & -\alpha_3 & a_2 \end{pmatrix}, \quad (2.5)$$

and

$$J_3 = \begin{pmatrix} \frac{\beta_1 S_0}{N} & 0 & \frac{\beta_3 S_0}{N} & \frac{\beta_2 S_0}{N} \\ -\gamma_1 & 0 & 0 & -\gamma_2 \end{pmatrix}, \quad J_4 = \begin{pmatrix} d & -\delta \\ 0 & d + \delta \end{pmatrix}, \quad (2.6)$$

we can get

$$R_0 = \rho(FV^{-1}) = \frac{\beta_1(a_2 a_3 - \alpha_1 \alpha_3) + \beta_3 \alpha \alpha_1 + \beta_2 a_3 \alpha}{a_1 a_2 a_3 - a_3 \alpha \alpha_4 - a_1 \alpha_1 \alpha_3}. \quad (2.7)$$

Consequently, we have the following conclusions

**Theorem 3.** The DFE of the model (2.2) is globally asymptotically stable if  $R_0 < 1$ .

**Proof** Model (2.2) can be rewritten as

$$\begin{pmatrix} \dot{E} \\ \dot{A} \\ \dot{I}_2 \\ \dot{I}_1 \end{pmatrix} = (F - V) \begin{pmatrix} E \\ A \\ I_2 \\ I_1 \end{pmatrix} - \left(1 - \frac{d}{\Lambda} S\right) F \begin{pmatrix} E \\ A \\ I_2 \\ I_1 \end{pmatrix}, \quad (2.8)$$

where  $F$  and  $V$  is given by (2.6), and from [28], we have

$$\begin{pmatrix} \dot{E} \\ \dot{A} \\ \dot{I}_2 \\ \dot{I}_1 \end{pmatrix} \leq (F - V) \begin{pmatrix} E \\ A \\ I_2 \\ I_1 \end{pmatrix}, \quad (2.9)$$

when  $t \rightarrow \infty$ ,  $S \rightarrow \frac{\Lambda}{d}$ ,  $(E, A, I_2, I_1) \rightarrow (0, 0, 0, 0)$ , that is,  $(S, R, E, A, I_2, I_1) \rightarrow x_0$  if  $t \rightarrow \infty$ .

Further,  $F$  is nonnegative,  $V$  is a nonsingular matrix and all eigenvalues of  $J_4$  have positive real part. According to [27], all eigenvalues of  $F - V$  have negative real part. Therefore, the DFE of the model (2.2) is globally asymptotically stable if  $R_0 < 1$ .

#### 2.4. Non-existence of limit cycles

**Theorem 4.** In the first quadrant, there is no limit cycle in system (2.2).

**Proof** We consider the Dulac function as  $B(S, E) = \frac{1}{SE}$ , now we have

$$\begin{aligned} \Theta &= \frac{\partial(BS)}{\partial S} + \frac{\partial(BE)}{\partial E} + \frac{\partial(BI_1)}{\partial I_1} + \frac{\partial(BI_2)}{\partial I_2} + \frac{\partial(BA)}{\partial A} + \frac{\partial(BR)}{\partial R} \\ &= \left( -\frac{\Lambda}{ES^2} - \frac{\delta R}{ES^2} \right) + \left( \frac{-\beta_2 I_1 N - \beta_3 I_2 N - \beta_1 E^2 - \beta_2 I_1 E - \beta_3 I_2 E}{(EN)^2} - \frac{\alpha_4 I_1}{ES^2} \right) \\ &\quad - \frac{\alpha_1 + \alpha_4 + \gamma_2 + d}{SE} - \frac{\alpha_3 + \alpha_2 + d}{SE} - \frac{\delta_1 + d}{SE} - \frac{\delta + d}{SE} \\ &< 0, \end{aligned}$$

therefore, by the Dulac–Bendixson theorem [29], there is no periodic orbit for the system (2.2).

#### 2.5. Existence of forward bifurcation

The epidemiological implications of backward bifurcation are that the effective disease control is only feasible if the basic reproduction number is reduced to values below another subthreshold less than unity [28]. Compared with backward bifurcation, the epidemiological significance of forward bifurcation means that the disease will disappear as long as the basic reproduction number is less than unity. Clearly, this phenomenon has important public health implications. Next, we analyze the existence and properties of bifurcation of the model.

Let

$$D_1 = \frac{a_2 a_3 - \alpha_1 \alpha_3}{\alpha \alpha_1} > 0, \quad D_2 = \frac{a_3}{\alpha_1}, \quad D_3 = \frac{\alpha_2}{a_4}, \quad D_4 = \frac{\gamma_1 (a_2 a_3 - \alpha_1 \alpha_3) + \gamma_2 \alpha a_3}{\alpha \alpha_1 a_5},$$

$$D_5 = \beta_1 D_1 + \beta_2 D_2 + D_3, \quad D_6 = 1 + D_1 + D_2 + D_3 + D_4,$$

$$D_7 = \frac{(a_1 D_1 - \alpha_4 D_2) D_6}{D_5 + \alpha_4 D_2 - a_1 D} = \frac{D_6}{R_0 - 1} > 0.$$

Setting the right-hand sides of model (2.2) to zero (at steady state) give by  $E_* = (S_*, E_*, I_{1*}, I_{2*}, A_*, R_*)$ , where

$$S_* = \frac{\Lambda R_0 D_7 (R_0 - 1)}{D_5 (R_0 - 1) + d D_6 R_0 - \delta R_0 (R_0 - 1) D_4}, \quad E_* = \frac{\Lambda R_0 D_1 (R_0 - 1)}{D_5 (R_0 - 1) + d D_6 R_0 - \delta R_0 (R_0 - 1) D_4},$$

$$I_{1^*} = \frac{\Lambda R_0 D_2 (R_0 - 1)}{D_5 (R_0 - 1) + dD_6 R_0 - \delta R_0 (R_0 - 1) D_4}, \quad I_{2^*} = \frac{\Lambda R_0 (R_0 - 1)}{D_5 (R_0 - 1) + dD_6 R_0 - \delta R_0 (R_0 - 1) D_4},$$

$$A_* = \frac{\Lambda R_0 D_3 (R_0 - 1)}{D_5 (R_0 - 1) + dD_6 R_0 - \delta R_0 (R_0 - 1) D_4}, \quad R_* = \frac{\Lambda R_0 D_4 (R_0 - 1)}{D_5 (R_0 - 1) + dD_6 R_0 - \delta R_0 (R_0 - 1) D_4}.$$

It is instructive to characterize the type of bifurcation the model (2.2) may undergo, and we demonstrate the results in Appendix A. This phenomenon is illustrated by simulating model (2.2) with the set of parameter values listed in Table 2. The associated forward bifurcation diagram, depicted in Figure 2, shows that the model has a disease-free equilibrium (corresponding to  $R_0 < 1$ ) (Figure 3) and an endemic equilibria (corresponding to  $R_0 > 1$ ) (Figure 4).

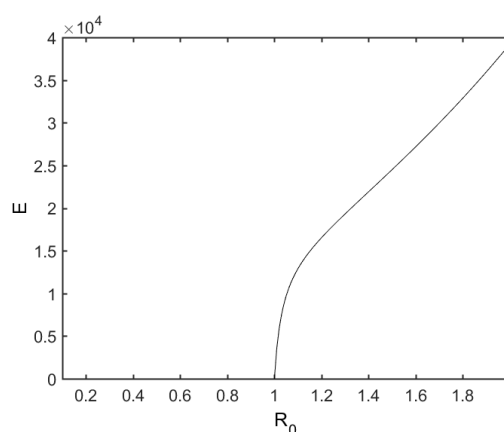


**Figure 2.** Forward bifurcation diagram of model (2.2).

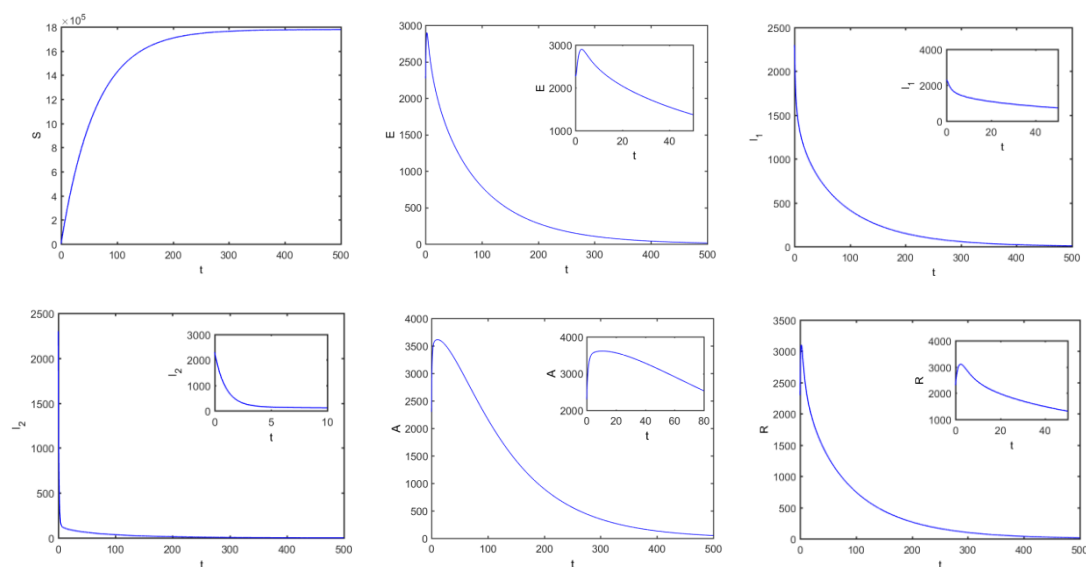


**Figure 3.** Changes of the every variable size over time, where  $\beta_1 = 0.1$ , and  $R_0 = 0.973$ .



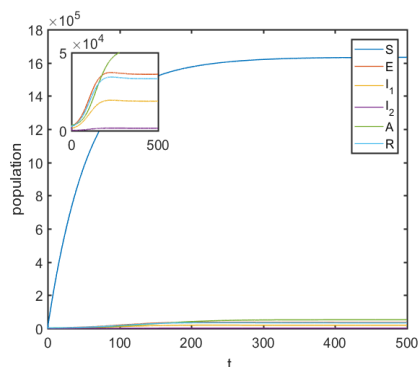


**Figure 4.** Changes of the every variable size over time, where  $\beta_1 = 0.16$  and  $R_0 = 1.0868$ .

**Table 2.** Values of the parameters.

Parameter	Value	Reference	Parameter	Value	Reference
$\Lambda$	28802	[30]	$\alpha_1$	0.09	[16]
$d$	0.0162	[30]	$\alpha_2$	0.57	[16]
$\delta_1$	0.001	[31]	$\alpha_3$	0.5	[33]
$\delta$	0.5	[16]	$\alpha_4$	0.000019	[33]
$\beta_1$	variable	Assumed	$\gamma_1$	0.0099	[16]
$\beta_2$	0.72	[31]	$\gamma_2$	0.891	[16]
$\beta_3$	0.81	[31]	$\alpha$	0.5	[32]

### 3. Efficacy of interventions and sensitivity analysis

#### 3.1. Efficacy of interventions

We used the parameter values given in Table 2 (unless otherwise stated) for our numerical simulations and changed the key parameter values to observe the corresponding effects on the disease outbreak.

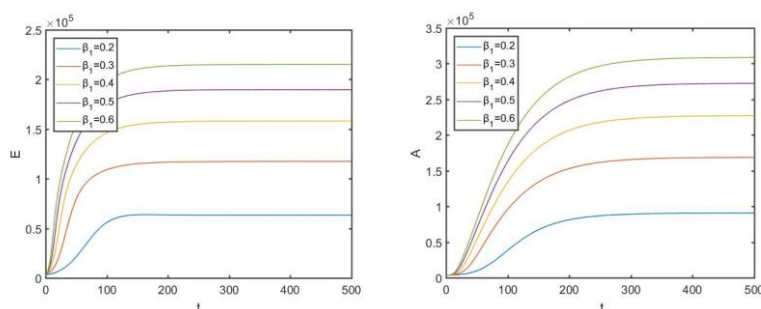


**Figure 5.** Variation in  $E(t)$ ,  $A(t)$  population with different parameters  $\beta_1$ .

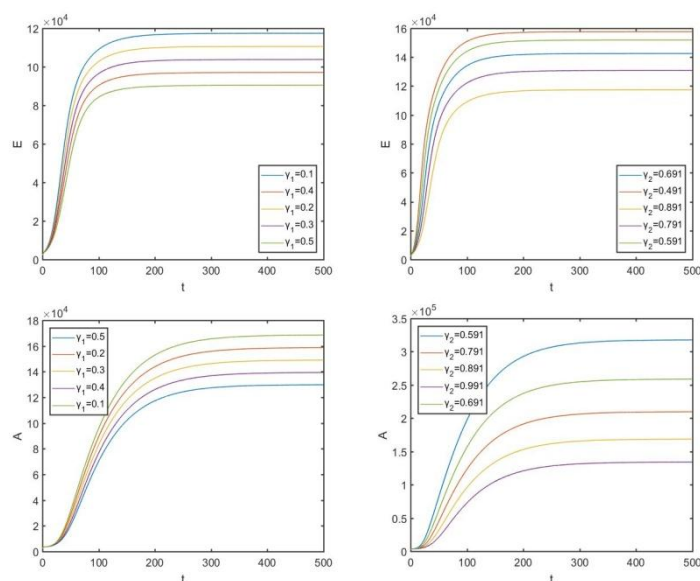


**Figure 6.** Variation in  $E(t)$ ,  $A(t)$  population with different parameters  $\gamma_1$ ,  $\gamma_2$ .

To investigate the effect of contact rate on disease infection, we varied  $\beta_1$ , as shown in Figure 5. The figure shows that as the contact rate of  $E(t)$  with  $S(t)$  increases, the number of infected individuals increases, and consequently, the increased contact rate will result in an increase in the disease outbreak.

To examine the effect of treatment rate on disease infection, we plotted Figure 6. It demonstrates that increasing the parameter  $\gamma_1$  and  $\gamma_2$  decreases the endemic levels of asymptomatic patients and cancer-infected individuals. In particular, if we increased treatment rate  $\gamma_1$  by 400%, the population of the asymptomatic patients and cancer-infected individuals would be decreased by 23%, and treatment rate  $\gamma_2$  would be increased by 68%. Finally, the endemic levels of the cancer-infected individuals population would be decreased by 58%. Moreover, increasing treatment rate  $\gamma_2$  by 81% would decrease the population of asymptomatic patients by 25%.

### 3.2. Sensitivity analysis of parameters in $R_0$

Latin hypercube sampling (LHS) is one of the Monte Carlo (MC) sampling methods that was first proposed by McKay [34] in 1979. The advantage of LHS sampling is that the number of iterations is less than in other methods of random sampling, and the clustering phenomenon of sampling is avoided [35].

Model (2.2) has 14 parameters. In order to identify the factors associated with a given intervention that most strongly affect the spread of a new infection, following [36] we performed Latin Hypercube Sampling on the parameters that appear in  $R_0$ . For the parameters in Eq. (2.7), Partial Rank Correlation Coefficients (PRCC) were calculated, and a total of 1000 simulations per LHS run were carried out. We chose a uniform distribution as the prior distribution when performing parameter sampling; the parameters of the model were set as input variables, and  $R_0$  as the output variable. If the absolute value of the PRCC is larger, the influence of the parameter in  $R_0$  is greater. It is assumed that if the  $p$  value is greater than 0.05, the parameter is not significant for  $R_0$ .

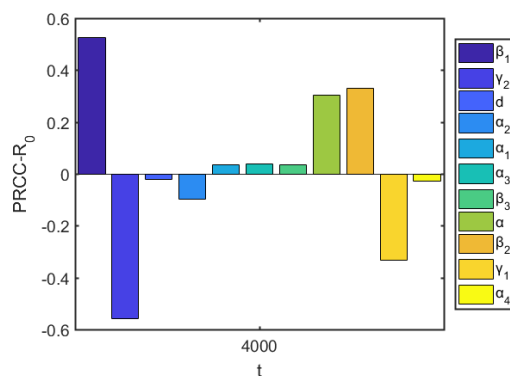


**Figure 7.** The sensitivity analysis of  $R_0$ .

**Table 3.** The range and PRCC values of the estimated parameters with respect to  $R_0$ .

Input parameter	Range	PRCC values	p-value
$\beta_1$	(0.01, 0.5)	0.526755	3.36E-143
$\gamma_2$	(0.3, 0.9)	-0.55735	1.29E-163
$d$	(0.005, 0.05)	-0.02163	0.333642
$\alpha_2$	(0.1, 0.9)	-0.09826	1.07E-05
$\alpha_1$	(0.01, 0.1)	0.034657	0.121282
$\alpha_3$	(0.1, 0.9)	0.039391	0.078208
$\beta_3$	(0.7, 0.99)	0.035278	0.114748
$\alpha$	(0.2, 0.8)	0.301851	2.09E-43
$\beta_2$	(0.5, 0.99)	0.33039	3.82E-52
$\gamma_1$	(0.4, 0.9)	-0.33434	1.98E-53
$\alpha_4$	(0.001, 0.01)	-0.02826	0.206432

Table 3 lists the PRCC values of the estimated parameters associated with  $R_0$ . The values reflect the correlation between the parameters  $\beta_1$ ,  $\gamma_2$ ,  $d$ ,  $\alpha_2$ ,  $\alpha_1$ ,  $\alpha_3$ ,  $\beta_3$ ,  $\alpha$ ,  $\beta_2$ ,  $\gamma_1$ ,  $\alpha_4$  and  $R_0$ . From Table 3 and Figure 7,  $\beta_1$ ,  $\alpha_1$ ,  $\alpha_3$ ,  $\beta_3$ ,  $\alpha$ ,  $\beta_2$  are positively correlated with  $R_0$ , while  $\gamma_2$ ,  $d$ ,  $\alpha_2$ ,  $\gamma_1$ ,  $\alpha_4$  are negatively correlated with  $R_0$ . Among the parameters, the positive influence of  $\beta_1$  and  $\beta_2$  on  $R_0$  is most obvious, that is, as  $\beta_1$  and  $\beta_2$  increase, the values of  $R_0$  increase rapidly, and more individuals will become infected. When symptomatic infectious individuals are continue to be infected and suffer from cancer, not only will the treatment be more difficult, the value of  $R_0$  will also increase. This indicates that the rate of progression to the symptomatic stage for individuals has a greater positive impact on  $R_0$ . In addition,  $\gamma_2$  and  $\gamma_1$  have the greatest negative impact on  $R_0$ , indicating that the value of  $R_0$  will decrease if the individuals with HPV symptoms or infectious individuals with no symptoms can be treated. Moreover, we can obtain that  $|PRCC(\gamma_2)| > |PRCC(\beta_1)| > |PRCC(\gamma_1)| > |PRCC(\beta_2)| > |PRCC(\alpha)|$ , namely,  $\gamma_2$ ,  $\beta_1$ ,  $\gamma_1$ ,  $\beta_2$ ,  $\alpha$ , play the most important roles in determining  $R_0$ .

### 3.3. Sensitivity analysis of parameters in infectious variables

Time-varying sensitivity explains the influence of parameters on state variables when they change with time [35], thereby evaluating the influence and dependence of parameters on state variables in dynamic models. Given the different outbreak time periods of various diseases, one should pay attention to the effect of time period. For example, after being infected with HPV, the clinical manifestations are diverse, and individuals can even be asymptomatic. Therefore, the entire time period of disease prevention, outbreak, infection, and treatment should be considered.

Based on the pathogenesis of HPV, this section considers the sensitivity analysis of parameters in state variables from two aspects, namely, a continuous period of time and a single point in time.

The sensitivity analysis of parameters in  $E(t)$  and  $A(t)$  in continuous time period is shown in Figure 8, we set parameters are input variables,  $E(t)$  and  $A(t)$  are output variables, the number of samples  $N = 2000$ .

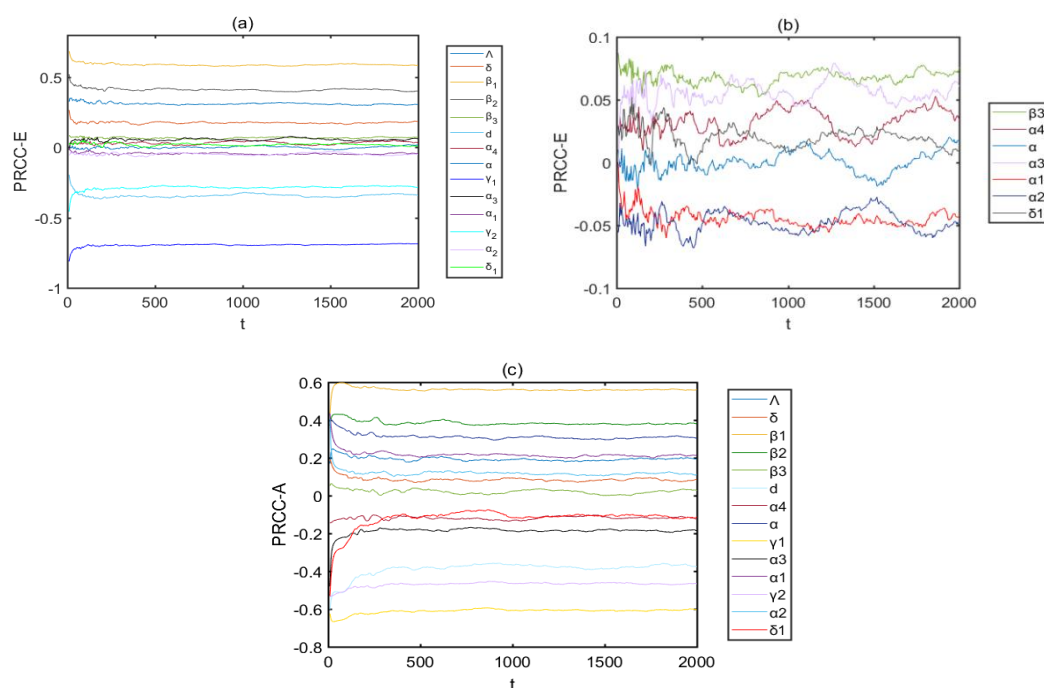


**Figure 8.** Sensitivity analysis of parameters in  $E(t)$  and  $A(t)$ .

In Figure 8, we show that the sensitivity of parameters in the early stages of disease outbreak changes significantly, especially before  $t = 500$ . As can be seen from Figure 8(a), the influence of  $\gamma_2$ ,  $\gamma_1$ ,  $\beta_1$ ,  $\beta_2$ ,  $d$  and  $\alpha$  has obvious changes, where the PRCC values of  $\gamma_2$  and  $\gamma_1$  decrease significantly with time, indicating that with the outbreak of disease, people have a certain understanding on the way of disease infection and have made great progress in the treatment. As the time increases, the treatment method quickly forms a treatment system, and it is difficult to progress within a short period of time, meaning that when  $t > 500$ , the influence of  $\gamma_2$  and  $\gamma_1$  is lessened. The PRCC values of  $\alpha$  have positive and negative fluctuations over time, indicating that in addition to the factors for abandoning treatment due to economic or social discrimination, it is also affected by the use of condoms and other protective measures. There are obvious changes illustrated in Figure 8(c), when  $t < 500$ , the influence of the transmission coefficients and the disease-induced

mortality  $\delta_1$  gradually increase, while due to the improvement of medical intervention, the PRCC values of  $\alpha_3$ ,  $\alpha_1$  and  $\alpha_2$  decrease.

The influence of different parameters on state variables is also different at a certain time [37], so the influence of parameters on state variables at  $t = 4000$  is studied, and the numerical simulation results can be seen in Table 4, Table 5, Figure 9, Figure 10, and Figure 11.

**Table 4.** The PRCC values of the estimated parameters with respect to  $E(t)$  at  $t = 4000$ .

Parameter	PRCC values	p-value	Parameter	PRCC values	p-value
$\Lambda$	0.3064	9.93E-45	$\alpha$	-0.0123	0.5810
$\delta$	0.1807	3.81E-16	$\gamma_1$	-0.6967	1.48E-290
$\beta_1$	0.5745	5.13E-176	$\alpha_3$	0.0782	0.0005
$\beta_2$	0.4073	8.57E-81	$\alpha_1$	-0.0745	0.0009
$\beta_3$	0.0240	0.2831	$\gamma_2$	-0.2450	9.96E-29
$d$	-0.2801	2.19E-37	$\alpha_2$	-0.0567	0.0112
$\alpha_4$	0.0080	0.7208	$\delta_1$	0.0240	0.2836

**Table 5.** The PRCC values of the estimated parameters with respect to  $A(t)$  at  $t = 4000$ .

Parameter	PRCC values	p-value	Parameter	PRCC values	p-value
$\Lambda$	0.23116	1.14E-25	$\alpha$	0.31927	1.26E-48
$\delta$	0.16689	5.84E-14	$\gamma_1$	-0.63554	9.74E-227
$\beta_1$	0.53907	3.65E-151	$\alpha_3$	-0.14916	2.03E-11
$\beta_2$	0.42215	2.95E-87	$\alpha_1$	0.24989	7.50E-30
$\beta_3$	0.087454	9.00E-05	$\gamma_2$	-0.44721	6.17E-99
$d$	-0.40263	8.11E-79	$\alpha_2$	0.14316	1.26E-10
$\alpha_4$	-0.08243	0.000224	$\delta_1$	-0.14249	1.55E-10

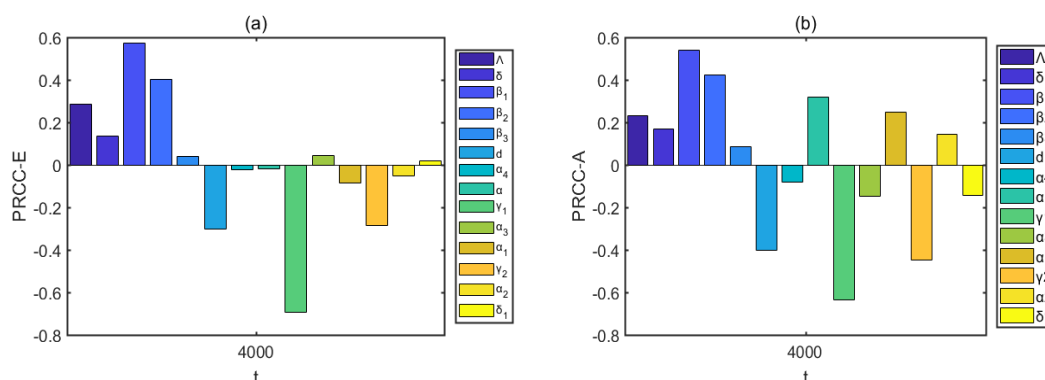


**Figure 9.** Sensitivity analysis of parameters in  $E(t)$  and  $A(t)$  at  $t = 4000$ .

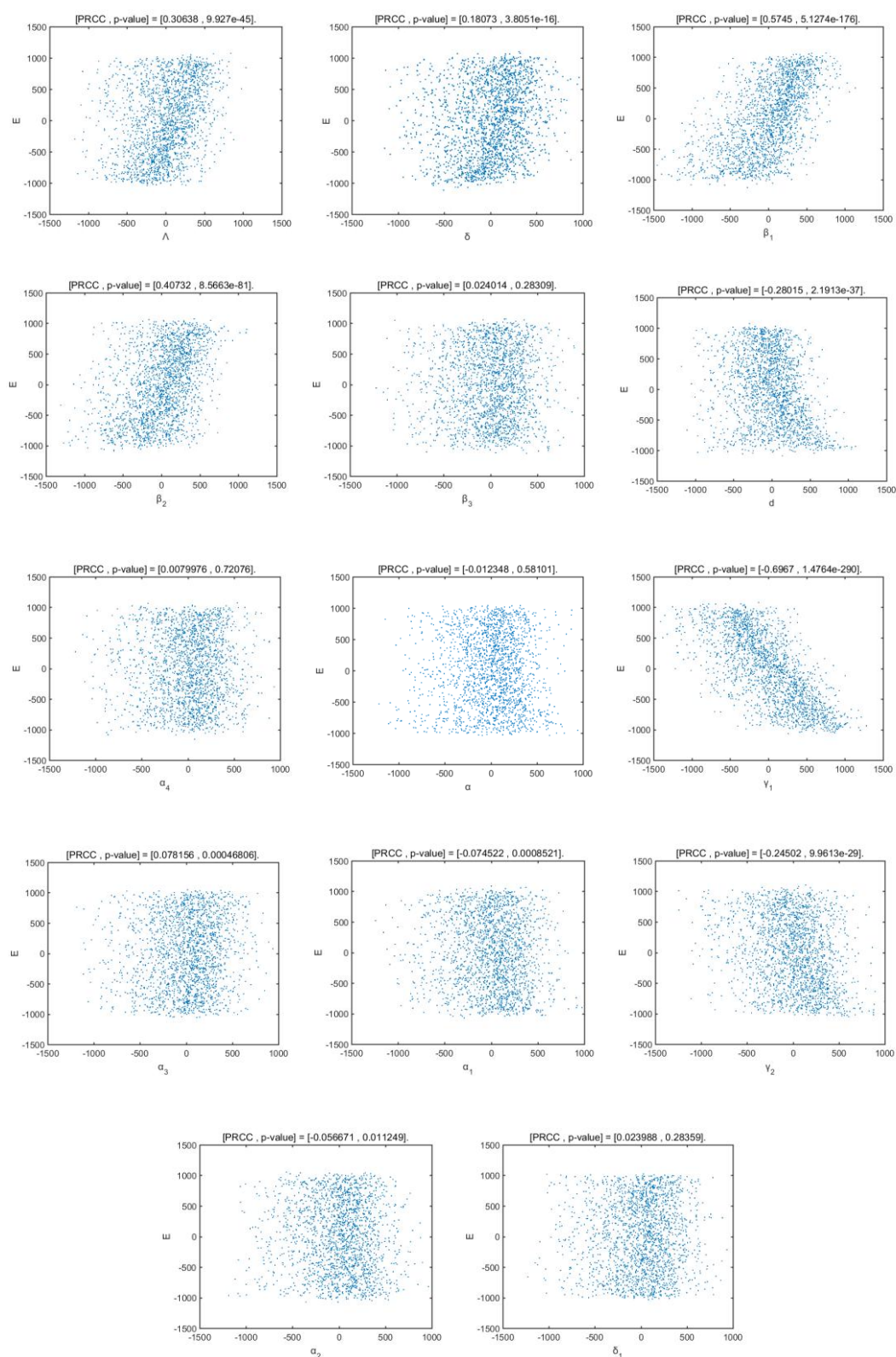


**Figure 10.** Scatter diagram of variable  $E(t)$  with respect to parameter PRCC values at  $t = 4000$ .

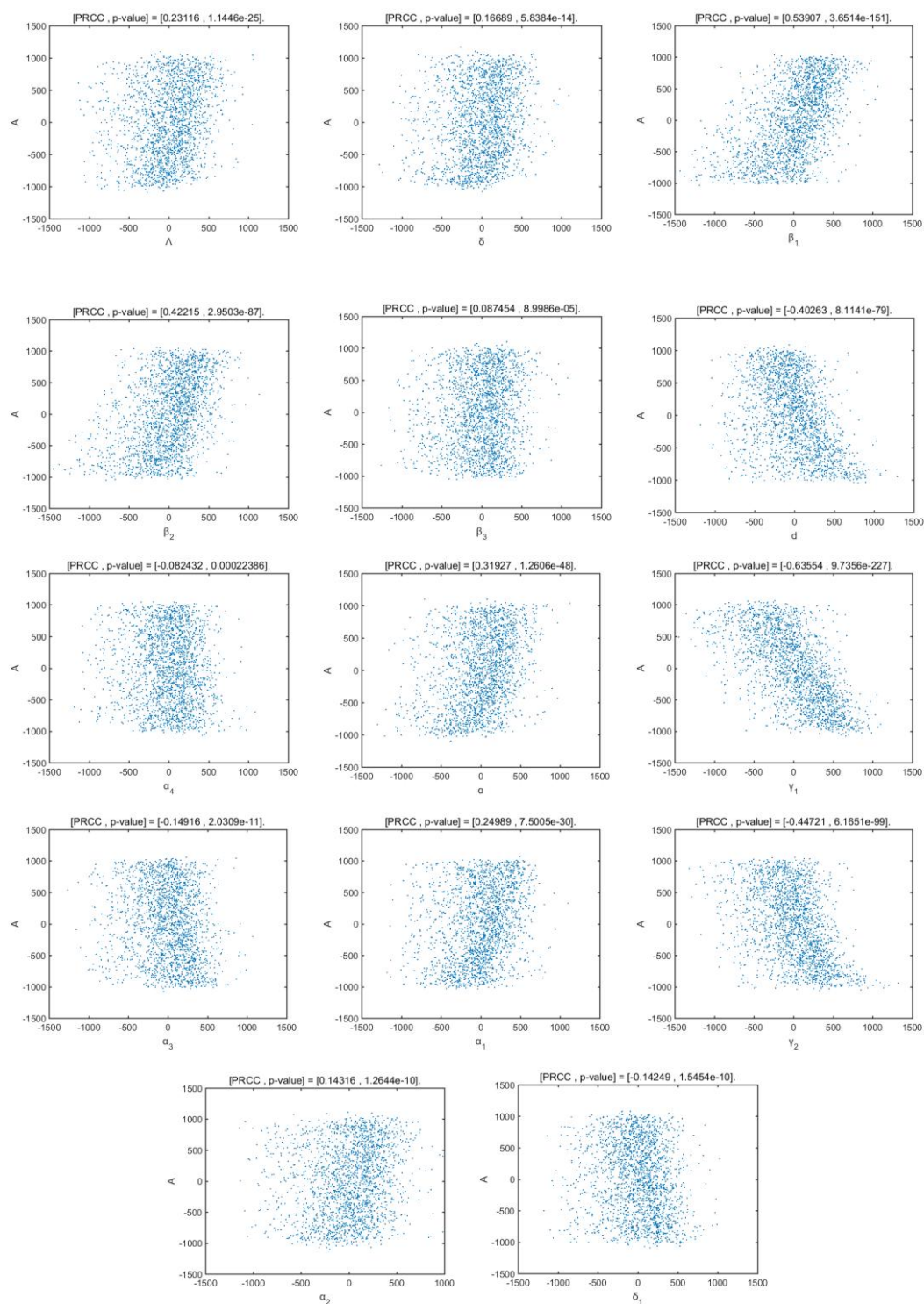


**Figure 11.** Scatter diagram of variable  $A(t)$  with respect to parameter PRCC values at  $t = 4000$ .

Figure 9 (a) and Table 4 shows that  $\beta_1$ ,  $\beta_2$  and  $E(t)$  are positively correlated, namely, the increase of  $\beta_1$ ,  $\beta_2$  will lead to the increase of  $E(t)$ ; while  $\gamma_1$ ,  $\gamma_2$  and  $E(t)$  have a significant negative correlation. Moreover, from Figure 10, we can get that the monotonicity of parameters  $\gamma_2$ ,

$\beta_1$ ,  $\beta_2$ ,  $\Lambda$  and  $d$  is most significant, in other words,  $E(t)$  is mainly affected by these parameters at this time.

From Figure 11 and Table 5, the monotonicity of parameter  $\beta_1$ ,  $\beta_2$ ,  $\gamma_1$ ,  $\gamma_2$ ,  $d$ ,  $\alpha_1$  and  $\alpha$  is obvious, from Figure 9 (b),  $\beta_1$ ,  $\beta_2$ ,  $\alpha$ ,  $\alpha_1$  has a positive correlation with  $A(t)$ , while  $\gamma_1$ ,  $\gamma_2$ ,  $d$  has a negative correlation with  $A(t)$ , which means that at this time, with the increase of  $\beta_1$ ,  $\beta_2$ ,  $\alpha$ ,  $\alpha_1$ , the number of  $A(t)$  will increase, but when  $\gamma_1$ ,  $\gamma_2$ ,  $d$  increases, the number of  $A(t)$  will decrease.

#### 4. Optimal control of the extended model

The spread of infectious diseases can be controlled through reasonable treatment [16]. In this section, the optimal treatment problem will be addressed within the framework of the optimal control problem for constraints [21].

##### 4.1. Formulation of the optimal treatment problem

We recorded  $\gamma_1$  as  $u$ , and indicated the rate of people receiving treatment in  $E(t)$ . Then an additional variable  $V(t)$  was introduced:

$$\dot{V} = uE, \quad (4.1)$$

where the value of  $V(t)$  at the initial time was set to 0. According to the actual situation, the treatment capacity of a city or a country is limited, and the number of people who can be treated is limited as well [38], so the following formula can be established as

$$u(t)E(t) < \Omega_1(t), \quad (4.2)$$

where  $\Omega_1(t)$  is the time-dependent upper limit of the number of people that can be treated at each time instant. In addition, state restrictions can be introduced to keep the asymptomatic patients population at a low level, according to [39] we proposed the following constraints

$$E(t) < E_{\max}, \quad (4.3)$$

where  $E_{\max}$  is the upper limit of  $E(t)$ .

Let  $x = [S, E, I_1, I_2, A, R]^T$ , and the treatment rate  $u(t)$ , was taken as the control variable. As to the cost function, the state variables and control variables are quadratic functions, which consider both the treatment rate and the number of asymptomatic patients. Based on the above description, the optimal treatment strategy can be formulated as the following problems with inequality constraints and free terminal state:



$$\text{Problem (P)} \left\{ \begin{array}{l} \min J = \int_0^{t_f} (A_1 E^2 + u^2) dt, \\ \text{s.t.} \\ \dot{S} = \Lambda + \delta R(t) - \lambda(t) S(t) - dS(t), \\ \dot{E} = \lambda(t) S(t) + \alpha_4 I_1(t) - (\alpha + u(t) + d) E(t), \\ \dot{I}_1 = \alpha E(t) + \alpha_3 I_2(t) - (\alpha_1 + \alpha_4 + \gamma_2 + d) I_1(t), \\ \dot{I}_2 = \alpha_1 I_1(t) - (\alpha_3 + \alpha_2 + d) I_2(t), \\ \dot{A} = \alpha_2 I_2(t) - (\delta_1 + d) A(t), \\ \dot{R} = u(t) E(t) + \gamma_2 I_1(t) - (\delta + d) R(t), \\ S(0) = S_s, E(0) = E_s, I_1(0) = I_{1s}, \\ I_2(0) = I_{2s}, A(0) = A_s, R(0) = R_s, \\ 0 \leq u \leq u_{\max}, E \leq E_{\max}, uE \leq \Omega_1, \end{array} \right. \quad (4.4)$$

where  $t_f \in \mathbf{R}^+$  is the terminal time;  $A_1 \in \mathbf{R}^+$  is the weight coefficient of  $E(t)$ .

#### 4.2. Analysis of optimal controls

The optimal control of the problem (P) is expressed as  $u_*$ . Next, we use the maximum principle of Pontryagin [21] to derive the optimal system for problem (P). Prior to this, we converted the inequality constraints in the problem (P) into equality constraints with some non-negative parameter parameters  $\eta_i$  ( $i = 1, 2, 3, 4$ ):

$$\left\{ \begin{array}{l} -u + \eta_1 = 0, \\ u - u_{\max} + \eta_2 = 0, \\ E - E_{\max} + \eta_3 = 0, \\ uE - \Omega_1 + \eta_4 = 0, \end{array} \right. \quad (4.5)$$

and we denoted  $\eta = [\eta_1, \eta_2, \eta_3, \eta_4]^T$ . Therefore, the Hamilton function of the problem (P) was obtained as follows

$$\begin{aligned} H = & A_1 E^2 + u^2 + \varphi_S (\Lambda + \delta R - \lambda S - dS) + \varphi_E [\lambda S + \alpha_4 I_1 - (\alpha + u(t) + d) E] \\ & + \varphi_{I_1} [\alpha E - \alpha_3 I_2 - (\alpha_1 + \alpha_4 + \gamma_2 + d) I_1] + \varphi_{I_2} [\alpha_1 I_1 - (\alpha_3 + \alpha_2 + d) I_2] \\ & + \varphi_A [\alpha_2 I_2 - (\delta_1 + d) A] + \varphi_R [u(t) E + \gamma_2 I_1 - (\delta + d) R] \\ & + \mu_1 (-u + \eta_1) + \mu_2 (u - u_{\max} + \eta_2) + \mu_3 (E - E_{\max} + \eta_3) + \mu_4 (uE - \Omega_1 + \eta_4), \end{aligned} \quad (4.6)$$

where  $\varphi = [\varphi_S, \varphi_E, \varphi_{I_1}, \varphi_{I_2}, \varphi_A, \varphi_R]^T$  are costate variables,  $\mu = [\mu_1, \mu_2, \mu_3, \mu_4]^T$  are non-negative penalty multipliers.

By using Pontryagin's maximum principle, the first-order necessary conditions can be obtained. The optimality conditions with respect to state, costate and parametric variables generate a two-point boundary value problem coupled with a nonlinear complementarity problem [21] as follow:

$$\dot{x} = \frac{\partial H}{\partial \varphi}, \quad (4.7)$$

$$\dot{\varphi} = -\frac{\partial H}{\partial x}, \quad (4.8)$$

and  $\eta \geq 0$ ,  $\mu \geq 0$ ,  $\eta^T \mu = 0$ .

Consider the optimality conditions with respect to the control variable

$$\frac{\partial H}{\partial u} = 0, \quad (4.9)$$

and from Eq. (4.8), the adjoint system can be derived as follow:

$$\begin{cases} \dot{\varphi}_S = (\varphi_S - \varphi_E) \left[ \frac{(\beta_1 E + \beta_2 I_1 + \beta_3 I_2)(N - S)}{N^2} \right] + \varphi_S d, \\ \dot{\varphi}_E = (\varphi_S - \varphi_E) \left[ \frac{\beta_1 S N - (\beta_1 S E + \beta_2 S I_1 + \beta_3 S I_2)}{N^2} \right] + \varphi_E a_1 - \varphi_{I_1} \alpha - \varphi_R u - \mu_3 - \mu_4 u - 2A_1 E, \\ \dot{\varphi}_{I_1} = (\varphi_S - \varphi_E) \left[ \frac{\beta_2 S N - (\beta_1 S E + \beta_2 S I_1 + \beta_3 S I_2)}{N^2} \right] - \varphi_E \alpha_4 + \varphi_{I_1} a_2 - \varphi_{I_2} \alpha_1 - \varphi_R \gamma_2, \\ \dot{\varphi}_{I_2} = (\varphi_S - \varphi_E) \left[ \frac{\beta_3 S N - (\beta_1 S E + \beta_2 S I_1 + \beta_3 S I_2)}{N^2} \right] - \varphi_{I_1} \alpha_3 + \varphi_{I_2} a_3 - \varphi_A \alpha_2, \\ \dot{\varphi}_A = \varphi_A a_4, \\ \dot{\varphi}_R = \varphi_R a_5 - \varphi_S \delta, \end{cases} \quad (4.10)$$

with the transversality conditions

$$\varphi_S(t_f) = \varphi_E(t_f) = \varphi_{I_1}(t_f) = \varphi_{I_2}(t_f) = \varphi_A(t_f) = \varphi_R(t_f) = 0.$$

From (4.4) we had  $0 \leq u \leq u_{\max}$  and  $u \leq \frac{\Omega_1}{E}$ , in other words,  $0 \leq u \leq \left\{ u_{\max}, \frac{\Omega_1}{E} \right\}$  is required

to be satisfied. Let  $u_{\max} = 1$  and  $\Omega_1 < E_{\max}$ . Hence,  $\frac{\Omega_1}{E} < u_{\max}$  always establishes.

By solving (4.9), we got

$$u_* = \frac{\varphi_E E + \mu_1 - \varphi_R E - \mu_2 - \mu_4 E}{2}. \quad (4.11)$$

We considered the case of  $\frac{\Omega_1}{E} > u_{\max}$ , under this assumption,  $u_* < \frac{\Omega_1}{E}$  always establishes,

therefore,  $\mu_4 = 0$ . Next, to determine the explicit expression of optimal control without  $\mu_1$  and  $\mu_2$ , we considered the following three assumptions:

(1) On the set  $\{t | 0 < u_* < u_{\max}\}$ , we had  $\mu_1 = \mu_2 = 0$ , hence,  $u_* = \frac{(\varphi_E - \varphi_R)E}{2}$ .

(2) On the set  $\{t | u_* = 0\}$ , we had  $\mu_2 = 0$ , therefore,  $0 = u_* = \frac{(\varphi_E - \varphi_R)E + \mu_1}{2}$ , and  $\mu_1 \geq 0$ , it is

determined that  $(\varphi_E - \varphi_R)E \leq 0$ .

(3) On the set  $\{t|u_* = u_{\max}\}$ , we had  $\mu_1 = 0$ , hence,  $u_* = u_{\max} = \frac{(\varphi_E - \varphi_R)E - \mu_2}{2}$ , and  $\mu_2 \geq 0$ , it is determined that  $\frac{(\varphi_E - \varphi_R)E}{2} \geq u_{\max}$ .

Combining the above three cases, the optimal control  $u_*$  is characterized as

$$u_* = \max \left\{ 0, \min \left\{ \frac{(\varphi_E - \varphi_R)E}{2}, u_{\max} \right\} \right\}.$$

Using the similar arguments, we can characterize the optimal control  $u_*$  under the condition where  $\frac{\Omega_1}{E} \leq u_{\max}$  as

$$u_* = \max \left\{ 0, \min \left\{ \frac{(\varphi_E - \varphi_R)E}{2}, \frac{\Omega_1}{E_*} \right\} \right\},$$

from the above discussions, an analytical expression of the optimal treatment rate is derived

$$u_* = \max \left\{ 0, \min \left\{ \frac{(\varphi_E - \varphi_R)E}{2}, u_{\max}, \frac{\Omega_1}{E} \right\} \right\}. \quad (4.12)$$

### 4.3. Numerical simulations

In this section, the symplectic pseudospectral method (SPM) developed in [40,41] is used to conduct numerical simulation. It owns structure-preserving property since the inherent Hamiltonian structure of optimal control problems is utilized. The local pseudospectral discretization scheme and the successive convexification technique are incorporated to make the algorithm fast and accurate. On one hand, the SPM can precisely quantify the energy variation for mechanical systems in optimal control and is thus widely used in vehicle trajectory planning [42–44]. On the other hand, it has sound stability for optimal control problems with long time span, which makes it an attractive method to solve policy-making problems for biological system [21].

When using the SPM in this section, the whole time span is divided into 10 regular sub-intervals and a 10-order approximation polynomial is used in each sub-interval. The parameters for the optimal control problem is set as Table 2 (unless otherwise stated in Table 6).

**Table 6.** Parameters and their values used in the simulation.

Parameter	Parameter description	Value
$\beta_1$	-	0.025
$\beta_2$	-	0.072
$\beta_3$	-	0.081
$\Omega_1$	Maximum treatment supply at each time instant	2000
$E_{\max}$	Maximum exposed population	2800
$u_{\max}$	Maximum treatment rate	1
$t_f$	Number of years	40
$A_1$	Weight on the asymptomatic patients population	0.002

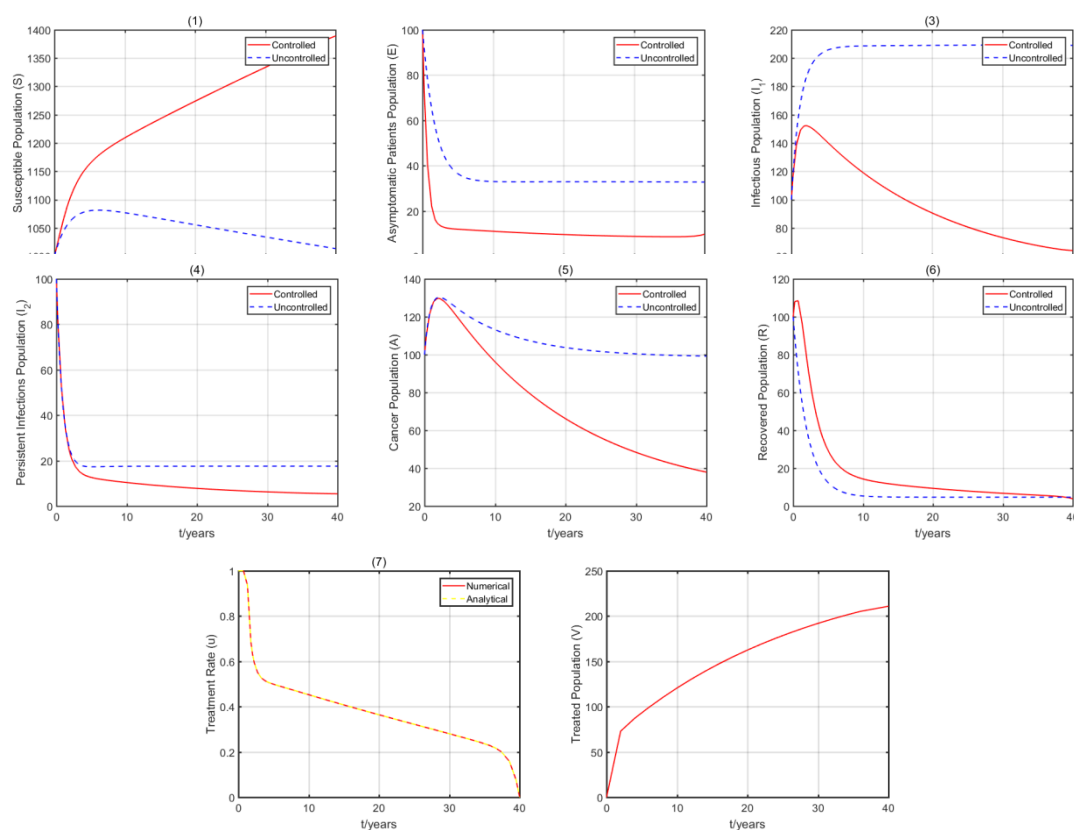


**Figure 12.** Optimal state trajectories, including (1) the susceptible population, (2) the asymptomatic patient population, (3) the infectious population, (4) the persistent infectious population, (5) the cancer population, (6) the recovered population, (7) Optimal treatment rate and (8) the treated population.

The controlled solution is shown in Figure 12 along with the uncontrolled solution. It can be seen that the treatment strategy is effective,  $I_1$  and  $A$  decreases rapidly and almost reaches zero at  $t = 40$ , and the values of  $E$  and  $I_2$  are also significantly reduced compared to before the addition of the treatment strategy. In addition, the values of  $S$  and  $R$  increased at the initial stage, and the effect before adding the treatment strategy is very obvious compared with the effect after the addition.

In the controlled case, the control variable  $u(t)$  is continuously reduced and reaches zero at the terminal. It can be seen from Figure 12(7) that the numerical solution of the control variable is in good agreement with the analytical solution given in (4.12), which verifies the characteristics of the optimal control.

## 5. Conclusion

For humans and some social animals, the standard incidence rate is more realistic than the bilinear incidence rate, so we used the standard incidence rate to indicate the ability of an infected person to infect others. Moreover, we assumed that the patients with persistent infection of HPV could be controlled and that mild infection could be cured, thus, those who are cured or have self-healed will gain immunity. Next, we established the model and analyzed its properties. It can be

seen from the analysis results that controlling the value of the parameter in  $R_0$ , making  $R_0$  less than 1, the disease will be die out, and when  $R_0$  greater than 1, the infection will experience an outbreak and form an endemic disease. The sensitivity analysis of the parameters in  $R_0$  and state variables illustrates that the value of  $R_0$  can be reduced or increased more efficiently, and the results can be used to control the spread of HPV. In the last section, the treatment rate is selected as the control variable, and the optimal treatment strategy is analyzed theoretically and simulated numerically. The results show that the appropriate treatment strategy can efficiently reduce the spread of the disease.

## Acknowledgments

This work was supported by the Fundamental Research Funds for the Central Universities (31920200037; 31920200070), the National Natural Science Foundation of China (31560127), the Program for Yong Talent of State Ethnic Affairs Commission of China (No. [2014]121), and Gansu Provincial First-class Discipline Program of Northwest Minzu University (No. 11080305).

## Conflict of interest

The authors declare that no conflict of interest.

## References

1. J. G. Baseman, L. A. Koutsky. *The epidemiology of human papillomavirus infections*, J. Clin. Virol., **32** (2005), 16–24.
2. F. X. Bosch, A. Lorincz, N. Munoz, et al. *The causal relation between human papillomavirus and cervical cancer*, J. Clin. Pathol., **55** (2002), 244–265.
3. D. Parkin, F. Bray, J. Ferlay, et al. *Estimating the world cancer burden: Globocan 2000*, Int. J. Cancer, **94** (2001), 153–156.
4. D. M. Parkin, F. Bray, J. Ferlay, et al. *Global cancer statistics, 2002*, CA: A Cancer Journal for Clinicians, **55** (2005), 74–108.
5. L. Bruni, M. Diaz, X. Castellsagué et al. *Cervical human papillomavirus prevalence in 5 continents: meta-analysis of 1 million women with normal cytological findings*, The Journal of Infections Disease, **202** (2010), 1789–1799.
6. D. Foreman, C. de Martel, C. J. Lacey, et al. *Global burden of human papillomavirus and related diseases*, Vaccine, **30** (2012), F12–F23.
7. F. X. Bosch, A. Lorincz, N. Munoz, et al. *The causal relation between human papillomavirus and cervical cancer*, J. Clin. Pathol., **55** (2002), 244–265.
8. J. M. Walboomers, M. V. Jacobs, M. M. Manos, et al. *Human papillomavirus is a necessary cause of invasive cervical cancer worldwide*, The Journal of Pathology, **189** (1999), 12–19.
9. K. Syrjanen, M. Hakama, S. Saarikoski, et al. *Prevalence, incidence, and estimated life-time risk of cervical human papillomavirus infections in a nonselected Finnish female population*, Sex. Transm. Dis., **17** (1990), 15–19.
10. G. Y. F. Ho, R. Bierman, L. Beardsley, et al. *Natural history of cervicovaginal papillomavirus infection in young women*, New Engl. J. Med., **338** (1998), 423–428.

11. A. B. Mosciki, S. Shiboski, J. Broering, et al. *The natural history of human papillomavirus infection as measured by repeated DNA testing in adolescent and young women*, Journal of Pediatrics, **2** (1998), 277–284.
12. S. B. Cantor, E. N. Atkinson, M. Cardenas-Turanzas, et al. *Natural history of cervical intraepithelial neoplasia: a meta-analysis*, Acta Cytol., **49** (2005), 405–415.
13. H. W. Chesson, J. M. Blandford, T. L. Gift, et al. *The estimated direct medical costs of sexually transmitted diseases among American youth, 2000*, Perspect Sex Reprod Health, **6** (2004), 11–19.
14. H. N. Coleman, W. W. Greenfield, S. L. Stratton, et al. *Human papillomavirus type 16 viral load is decreased following a therapeutic vaccination*, Cancer Immunol Immunother, **65** (2016), 563–573.
15. H. Gemma, H. Karin, D. Lucy, *Therapeutic HPV vaccines*, Best Practice & Research Clinical Obstetrics and Gynaecology, **47** (2018), 59–72.
16. A. Oname, R. A. Umana, D. Okuonghae, et al. *Mathematical analysis of a two-sex Human Papillomavirus (HPV) model*, Int. J. Biomath., **7** (2018), 43.
17. Elamin H, Elbasha, E. J. Dasbach, R. P. Insinga, *A Multi-Type HPV Transmission Model*, B. Math. Biol., **70** (2008), 2126–2176.
18. Elamin H, Elbasha, *Global Stability of Equilibria in a Two-Sex HPV Vaccination Model*, B. Math. Biol., **70** (2008), 894–909.
19. A. Mo'tassem, S. Robert, *An age-structured model of human papilloma virus vaccination*, Math. Comput. Simulat., **82** (2011), 629–652.
20. E. B. M. Bashier, K. C. Patidar, *Optimal control of an epidemiological model with multiple time delays*, Appl. Math. Comput., **292** (2017), 47–56.
21. X. Wang, H. Peng, S. Yang, et al. *Optimal vaccination strategy of a constrained time-varying SEIR epidemic model*, Commun. Nonlinear Sci., **67** (2019), 37–48.
22. T. K. Kar, AshimBatabyal, *Stability analysis and optimal control of an SIR epidemic model with vaccination*, Biosystems, **104** (2011), 127–135.
23. Y. Yang, S. Y. Tang, X. H. Ren, et al. *Global stability and optimal control for a tuberculosis model with vaccination and treatment*, Discrete and continuous dynamical systems series B, **21** (2016), 1009–1022.
24. F. X. Bosch, A. Lorincz, N. Munoz, et al. *The causal relation between human papillomavirus and cervical cancer*, J. Clin. Pathol., **55** (2002), 244.
25. S. Lakshmikantham, S. Leela, A. A. Martynyuk, *Stability Analysis of Nonlinear Systems*, Marcel Dekker, New York. 1989.
26. H. W. Hethcote, *The mathematics of infectious diseases*, Siam Rev., **42** (2000), 599–653.
27. P. van den Driessche, J. Watmough, *Reproduction numbers and sub-threshold endemic equilibria for compartmental models of disease transmission*, Math. Biosci., **180** (2002), 29–48.
28. O. Sharomi, C. N. Podder, A. B. Gumel, et al. *Modelling the Transmission Dynamics and Control of Novel 2009 Swine Influenza (H1N1) Pandemic*, B. Math. Biol., **73** (2011), 515–548.
29. L. Perko, *Differential Equations and Dynamical Systems*, Springer, New York, 1996.
30. CIA World Factbook, South Africa Demographics Profile, 2016.
31. M. T. Malik, J. Reimer, A. B. Gumel, et al. *The impact of an imperfect vaccine and pap cytology screening on the transmission of human papillomavirus and occurrence of associated cervical dysplasia and cancer*, Math. Biosci. Eng., **10** (2013), 1173–1205.
32. A. A. Alsaleh, A. B. Gumel, *Dynamics of a vaccination model for HPV transmission*, J. Biol. Syst., **22** (2014), 555–599.

33. A. A. Alsaleh, A. B. Gumel, *Analysis of a risk-structured vaccination model for the dynamics of oncogenic and warts-causing HPV types*, *B. Math. Biol.*, **76** (2014), 1670–1726.
34. H. Huo, L. X. Feng, *Global stability for an HIV/AIDS epidemic model with different latent stages and treatment*, *Appl. Math. Model.*, **37** (2013), 1480–1489.
35. M. Simeone, B. H. Ian, J. R. Christian, et al. *A methodology for performing global uncertainty and sensitivity analysis in systems biology*, *J. Theor. Biol.*, **254** (2008), 178–196.
36. S. M. Blower, H. Dowlatabadi, *Sensitivity and uncertainty analysis of complex models of disease transmission: An HIV model, as an example*, *Int. Stat. Rev.*, **2** (1994), 229–243.
37. R. Jan, Y. N. Xiao, *Effect of partial immunity on transmission dynamics of dengue disease with optimal control*, *Mathematical Methods in the Applied Sciences*, **42** (2019), 1967–1983.
38. W. Wang, *Backward bifurcation of an epidemic model with treatment*, *Math. Biosci.*, **201** (2016), 58–71.
39. M. H. A. Biswas, L. T. Paiva, M. Do Rosario de Pinho, *A SEIR model for control of infectious diseases with constraints*, *Math. Biosci. Eng.*, **11** (2014), 761–784.
40. H. Peng, X. Wang, B. Shi, et al. *Stabilizing constrained chaotic system using a symplectic pseudospectral method*, *Commun. Nonlinear Sci.*, **56** (2018), 77–92.
41. X. Wang, H. Peng, S. Zhang, et al. *A symplectic pseudospectral method for nonlinear optimal control problems with inequality constraints*, *ISA T.*, **68** (2017), 335–352.
42. X. Wang, J. Liu, Y. Zhang, et al. *A unified symplectic pseudospectral method for motion planning and tracking control of 3D underactuated overhead cranes*, *International Journal of Robust Nonlinear Control*, **29** (2019), 2236–2253.
43. X. Wang, H. Peng, D. Jiang, et al. *Optimal Path Planning of Two-Wheeled Mobile Robots in the Presence of Dynamic Obstacles*, *The 36th Chinese Control Conference*, IEEE, 2017.
44. J. Liu, W. Han, X. Wang, et al. *Research on Cooperative Trajectory Planning and Tracking Problem for Multiple Carrier Aircraft on the Deck*, *IEEE System Journal*, 2019.
45. C. Castillo-Chavez, B. Song, *Dynamical models of tuberculosis and their applications*, *Math. Biosci. Eng.*, **2** (2004), 361–404.
46. J. Carr, *Applications Centre Manifold Theory*, New York: Springer, 1981.

## Appendix A

**Proof** The existence of forward bifurcation will be explored using the Centre Manifold Theory [27,45,46]. To apply this theory, it is necessary to carry out the following change of variables.

Let  $S = x_1$ ,  $E = x_2$ ,  $I_1 = x_3$ ,  $I_2 = x_4$ ,  $A = x_5$ ,  $R = x_6$ , so that

$$N = \sum_{i=1}^6 x_i,$$

further, using the vector notation

$$X = (x_1, x_2, x_3, x_4, x_5, x_6)^T,$$

the model (2.2) can be re-written in the form

$$\frac{dX}{dt} = (f_1, f_2, f_3, f_4, f_5, f_6)^T,$$

as follows:

$$\left\{ \begin{array}{l} \frac{dx_1}{dt} = \Lambda + \delta x_6(t) - \lambda(t)x_1(t) - dx_1(t), \\ \frac{dx_2}{dt} = \lambda(t)x_1(t) + \alpha_4 x_3(t) - (\alpha + \gamma_1 + d)x_2(t), \\ \frac{dx_3}{dt} = \alpha x_2(t) + \alpha_3 x_4(t) - (\alpha_1 + \alpha_4 + \gamma_2 + d)x_3(t), \\ \frac{dx_4}{dt} = \alpha_1 x_3(t) - (\alpha_3 + \alpha_2 + d)x_4(t), \\ \frac{dx_5}{dt} = \alpha_2 x_4(t) - (\delta_1 + d)x_5(t), \\ \frac{dx_6}{dt} = \gamma_1 x_2 + \gamma_2 x_3 - (\delta + d)x_6(t). \end{array} \right. \quad (\text{A.1})$$

Consider the case when  $R_0=1$ . Suppose, further, that  $\beta_1$  is chosen as a bifurcation parameter. Solving for  $\beta_1 = \beta_1^*$  from  $R_0=1$  gives

$$\beta_1^* = \frac{a_1 a_2 a_3 - \beta_2 a_3 \alpha - a_3 \alpha \alpha_4 - a_1 \alpha_1 \alpha_3 - \beta_3 \alpha \alpha_1}{a_2 a_3 - \alpha_1 \alpha_3}. \quad (\text{A.2})$$

The Jacobian of the system (A.2) evaluated at the DFE is given as

$$J_{E_0} = \begin{pmatrix} -d & -\beta_1^* & -\beta_2 & -\beta_3 & 0 & \delta \\ 0 & \beta_1^* - a_1 & \beta_2 + \alpha_4 & \beta_3 & 0 & 0 \\ 0 & \alpha & -a_2 & \alpha_3 & 0 & 0 \\ 0 & 0 & \alpha_1 & -a_3 & 0 & 0 \\ 0 & 0 & 0 & \alpha_2 & -a_4 & 0 \\ 0 & \gamma_1 & \gamma_2 & 0 & 0 & -a_5 \end{pmatrix}.$$

It is easy to verify that the transformed system (A.2), with  $\beta_1 = \beta_1^*$ , has a hyperbolic equilibrium point (i.e., the linearized system has a simple eigenvalue with zero real part, and all other eigenvalues have negative real parts). Hence, the centre manifold theory can be used to analyse the dynamics of (A.2) near  $\beta_1 = \beta_1^*$ .

It can be shown that the Jacobian of (A.2) at  $\beta_1 = \beta_1^*$  has a right eigenvector (associated with the zero eigenvalue) given by  $w = (\omega_1, \omega_2, \omega_3, \omega_4, \omega_5, \omega_6)^T$ , where

$$\omega_1 = \frac{\delta [\gamma_1 a_1 \beta_3 + \gamma_1 a_3 (\beta_2 + \alpha_4) + \gamma_2 a_3 (a_1 - \beta_1^*)] - a_3 a_5 \beta_1^* \alpha_4 - a_1 a_3 a_5 \beta_2 - a_1^2 a_5 \beta_3}{a_5 (a_1 - \beta_1^*)},$$

$$\omega_2 = \frac{a_1 \beta_3 + a_3 (\beta_2 + \alpha_4)}{a_1 - \beta_1^*} > 0, \quad \omega_3 = a_3, \quad \omega_4 = a_1, \quad \omega_5 = \frac{a_1 \alpha_2}{a_4},$$

$$\omega_6 = \frac{\gamma_1 a_1 \beta_1^* + \gamma_1 a_3 (\beta_2 + \alpha_4) + \gamma_2 a_3 (a_1 - \beta_1^*)}{a_5 (a_1 - \beta_1^*)} > 0.$$



The components of the left eigenvector of  $J_{E_0}|_{\beta_1=\beta_1^*}$ ,  $v = (v_1, v_2, v_3, v_4, v_5, v_6)$ , satisfying  $v \cdot w = 1$  are

$$v_1 = v_5 = v_6 = 0,$$

$$v_2 = \frac{a_3 \alpha (a_1 - \beta_1^*)}{a_3 \alpha [a_1 \beta_3 + a_3 (\beta_2 + \alpha_4)] + a_3^2 (a_1 - \beta_1^*)^2 + a_1 (a_1 - \beta_1^*) [\alpha \beta_3 + \alpha_3 (a_1 - \beta_1^*)]} > 0,$$

$$v_3 = \frac{a_3 (a_1 - \beta_1^*)^2}{a_3 \alpha [a_1 \beta_3 + a_3 (\beta_2 + \alpha_4)] + a_3^2 (a_1 - \beta_1^*)^2 + a_1 (a_1 - \beta_1^*) [\alpha \beta_3 + \alpha_3 (a_1 - \beta_1^*)]} > 0,$$

$$v_4 = \frac{(a_1 - \beta_1^*) [\alpha \beta_3 + \alpha_3 (a_1 - \beta_1^*)]}{a_3 \alpha [a_1 \beta_3 + a_3 (\beta_2 + \alpha_4)] + a_3^2 (a_1 - \beta_1^*)^2 + a_1 (a_1 - \beta_1^*) [\alpha \beta_3 + \alpha_3 (a_1 - \beta_1^*)]} > 0,$$

It follows from [22,28,29], we have

$$a = \sum_{k,i,j=1}^6 v_k \omega_i \omega_j \frac{\partial^2 f_k}{\partial x_i \partial x_j}(0,0), \quad b = \sum_{k,i=1}^6 v_k \omega_i \frac{\partial^2 f_k}{\partial x_i \partial \beta_1}(0,0),$$

are computed to be

$$\begin{aligned} a = & -2v_2 \omega_2 \omega_2 \frac{\beta_1 d}{\Lambda} - v_2 \omega_2 \omega_3 \frac{(\beta_1 + \beta_2) d}{\Lambda} - v_2 \omega_2 \omega_4 \frac{(\beta_1 + \beta_3) d}{\Lambda} - v_2 \omega_2 \omega_5 \frac{\beta_1 d}{\Lambda} - v_2 \omega_2 \omega_6 \frac{\beta_1 d}{\Lambda} \\ & - v_2 \omega_3 \omega_2 \frac{(\beta_1 + \beta_2) d}{\Lambda} - 2v_2 \omega_3 \omega_3 \frac{\beta_2 d}{\Lambda} - v_2 \omega_3 \omega_4 \frac{(\beta_2 + \beta_3) d}{\Lambda} - v_2 \omega_3 \omega_5 \frac{\beta_2 d}{\Lambda} - v_2 \omega_2 \omega_5 \frac{\beta_2 d}{\Lambda} \\ & - v_2 \omega_4 \omega_2 \frac{(\beta_1 + \beta_3) d}{\Lambda} - v_2 \omega_4 \omega_3 \frac{(\beta_2 + \beta_3) d}{\Lambda} - 2v_2 \omega_4 \omega_4 \frac{\beta_3 d}{\Lambda} - v_2 \omega_4 \omega_5 \frac{\beta_3 d}{\Lambda} - v_2 \omega_4 \omega_6 \frac{\beta_3 d}{\Lambda} \\ & - v_2 \omega_5 \omega_2 \frac{\beta_1 d}{\Lambda} - v_2 \omega_5 \omega_3 \frac{\beta_2 d}{\Lambda} - v_2 \omega_5 \omega_4 \frac{\beta_3 d}{\Lambda} - v_2 \omega_6 \omega_2 \frac{\beta_1 d}{\Lambda} - v_2 \omega_6 \omega_3 \frac{\beta_2 d}{\Lambda} - v_2 \omega_6 \omega_4 \frac{\beta_3 d}{\Lambda} \\ < 0, \end{aligned} \tag{A.3}$$

$$b = v_2 \omega_2 > 0.$$

Since the bifurcation coefficient  $b$  is positive, it follows from theorem that the model (A.2) will undergo a forward bifurcation.



AIMS Press

© 2020 the Author(s), licensee AIMS Press. This is an open access article distributed under the terms of the Creative Commons Attribution License (<http://creativecommons.org/licenses/by/4.0>)